Molecular Human Reproduction, Vol.22, No.2 pp. 130–142, 2016
Advanced Access publication on December 7, 2015 doi:10.1093/molehr/gav069

molecular human reproduction

ORIGINAL RESEARCH

Placental growth factor deficiency is associated with impaired cerebral vascular development in mice

Rayana Leal Luna[1,2,†], Vanessa R. Kay[1,†], Matthew T. Rätsep[1], Kasra Khalaj[1], Mallikarjun Bidarimath[1], Nichole Peterson[1], Peter Carmeliet[3], Albert Jin[1], and B. Anne Croy[1,*]

[1]Department of Biomedical and Molecular Sciences, Queen's University, Kingston, ON K7L 3N6, Canada [2]Federal University of Pernambuco – UFPE, Recife, Pernambuco 50670-901, Brazil [3]Laboratory of Angiogenesis and Neurovascular Link, Vesalius Research Center, Department of Oncology, University of Leuven, Leuven, Belgium

*Correspondence address. 924 Botterell Hall, 18 Stuart St., Queen's University, Kingston, ON K7L 3N6, Canada. Tel: +1-613-533-2859; Fax: +1-613-533-2022; E-mail: croya@queensu.ca

Submitted on October 6, 2015; resubmitted on November 23, 2015; accepted on November 27, 2015

STUDY HYPOTHESIS: Placental growth factor (PGF) is expressed in the developing mouse brain and contributes to vascularization and vessel patterning.

STUDY FINDING: PGF is dynamically expressed in fetal mouse brain, particularly forebrain, and is essential for normal cerebrovascular development.

WHAT IS KNOWN ALREADY: PGF rises in maternal plasma over normal human and mouse pregnancy but is low in many women with the acute onset hypertensive syndrome, pre-eclampsia (PE). Little is known about the expression of PGF in the fetus during PE. *Pgf*$^{-/-}$ mice appear normal but recently cerebral vascular defects were documented in adult *Pgf*$^{-/-}$ mice.

STUDY DESIGN, SAMPLES/MATERIALS, METHODS: Here, temporal–spatial expression of PGF is mapped in normal fetal mouse brains and cerebral vasculature development is compared between normal and congenic *Pgf*$^{-/-}$ fetuses to assess the actions of PGF during cerebrovascular development. *Pgf*/PGF, *Vegfa*/VEGF, *Vegf* receptor (*Vegfr*)1 and *Vegfr2* expression were examined in the brains of embryonic day (E)12.5, 14.5, 16.5 and 18.5 C57BL/6 (B6) mice using quantitative PCR and immunohistochemistry. The cerebral vasculature was compared between *Pgf*$^{-/-}$ and B6 embryonic and adult brains using whole mount techniques. Vulnerability to cerebral ischemia was investigated using a left common carotid ligation assay.

MAIN RESULTS AND THE ROLE OF CHANCE: *Pgf*/PGF and *Vegfr1* are highly expressed in E12.5-14.5 forebrain relative to VEGF and *Vegfr2*. *Vegfa*/VEGF is relatively more abundant in hindbrain (HB). PGF and VEGF expression were similar in midbrain. Delayed HB vascularization was seen at E10.5 and 11.5 in *Pgf*$^{-/-}$ brains. At E14.5, *Pgf*$^{-/-}$ circle of Willis showed unilateral hypoplasia and fewer collateral vessels, defects that persisted post-natally. Functionally, adult *Pgf*$^{-/-}$ mice experienced cerebral ischemia after left common carotid arterial occlusion while B6 mice did not.

LIMITATIONS, REASONS FOR CAUTION: Since *Pgf*$^{-/-}$ mice were used, consequences of complete absence of maternal and fetal PGF were defined. Therefore, the effects of maternal versus fetal PGF deficiency on cerebrovascular development cannot be separated. However, as PGF was strongly expressed in the developing brain at all timepoints, we suggest that local PGF has a more important role than distant maternal or placental sources. Full PGF loss is not expected in PE pregnancies, predicting that the effects of PGF deficiency identified in this model will be more severe than any effects in PE-offspring.

WIDER IMPLICATIONS OF THE FINDINGS: These studies provoke the question of whether PGF expression is decreased and cerebral vascular maldevelopment occurs in fetuses who experience a preeclamptic gestation. These individuals have already been reported to have elevated risk for stroke and cognitive impairments.

LARGE SCALE DATA: N/A.

[†] These authors contributed equally.

STUDY FUNDING AND COMPETING INTEREST(S): This work was supported by awards from the Natural Sciences and Engineering Research Council, the Canada Research Chairs Program and the Canadian Foundation for Innovation to B.A.C. and by training awards from the Universidade Federal de Pernambuco and Conselho Nacional de Desenvolvimento Cientifico e Tecnologico (CNPq), Brazil to R.L.L.; Queen's University to V.R.K. and the Canadian Institutes of Health Research to M.T.R. The work of P.C. is supported by the Belgian Science Policy BELSPO—IUAP7/03, Structural funding by the Flemish Government—Methusalem funding, and the Flemish Science Fund—FWO grants. There were no competing interests.

Key words: cerebral vessels / circle of Willis / fetal development / PGF / pre-eclampsia / stroke

Introduction

Women who experience pre-eclampsia (PE), an acute hypertensive syndrome of pregnancy, are at increased cardiovascular disease risk later in life (Powers *et al.*, 2012). Fewer studies address effects of PE on offspring cardiovascular health. One long-term cohort study reported greater risk for stroke but not coronary heart disease in offspring of preeclamptic pregnancies aged 59–69 (Kajantie *et al.*, 2009). Elevated stroke sensitivity was postulated to result from reduced fetal brain growth or from a 'brain-sparing response' that redirected blood to the brain, permanently altering fetal cerebral vessels (Kajantie *et al.*, 2009). Genetic, epigenetic, and environmental factors that alter placental function are also proposed to decrease cardiovascular fitness in offspring of preeclamptic pregnancies (Davis *et al.*, 2012; Herrera-Garcia and Contag, 2014). Suboptimal placental production of angiogenic factors such as placental growth factor (PGF, previously PLGF) and/or increased release of anti-angiogenic proteins such as sFLT1 characterize PE (Powers *et al.*, 2012; Goel and Rana, 2013). While PGF deficiency precedes clinical signs of PE in many women, significant outcomes due to fetal PGF deficiency have not been investigated (Carmeliet *et al.*, 2001). However, PGF/*Pgf* expression is reported in human and mouse oocytes and in embryos from zygote to blastocyst stages (Gene Expression Omnibus database: GDS3958, GDS812 and GDS813) (Zeng *et al.*, 2004; Xie *et al.*, 2010). Thus, dysregulation of the angiogenic pathways that contribute to PE may begin prior to implantation and before placental lineage commitment in the blastocyst. If so, dysregulated angiogenesis would be predicted in both placental and inner cell mass-derived fetal tissues. Genetic or epigenetic factors affecting gene expression in the blastocyst lineages may also explain the higher risk of pre-eclampsia in subsequent pregnancies of women who have had pre-eclampsia (Hernández-Díaz *et al.*, 2009).

Like vascular endothelial growth factor-A (VEGF), PGF binds to membrane-bound and soluble forms of the FLT1 receptor (VEGFR1). However, only VEGF and not PGF binds to the Kinase insert domain receptor (KDR/VEGFR2) (Autiero *et al.*, 2003; Cao, 2009). Both VEGF receptors engage multiple co-receptors and participate in complex signaling pathways. Humans express four isoforms of PGF while mice only have one, which corresponds to the human PGF-2 (Dewerchin and Carmeliet, 2012). *Pgf*$^{-/-}$ mice are viable and develop apparently normally, resulting in a consensus that PGF is of limited importance developmentally or in maintenance of homeostasis but acts under disturbed states such as pregnancy, ischemic heart repair and tumor vessel induction (Dewerchin and Carmeliet, 2014). PGF is made not only by placenta but by other cell types such as endothelium and hepatocytes (Steenkiste *et al.*, 2011) and it can be induced in adult neurons, Schwann cells and astrocytes (Beck *et al.*, 2002; Hayashi *et al.*, 2003; Freitas-Andrade *et al.*, 2008; Chaballe *et al.*, 2011). Because PGF is a large glycoprotein (Christinger *et al.*, 2004; Errico *et al.*, 2004), maternal plasma PGF is unlikely to cross the placenta although it may induce signaling via placentally expressed VEGFR1s or neuropilins (NRP) (Baston-Buest *et al.*, 2011). Data on fetal PGF production are minimal. One study reported week 7–9 human amniotic fluid had a PGF concentration approximately half that of matched maternal serum (Makrydimas *et al.*, 2008). Over midgestation, PGF and VEGF levels increase in amniotic fluid with VEGF at a 6-fold greater concentration than PGF (Kalampokas *et al.*, 2012; Papapostolou *et al.*, 2012). At term, PGF is generally undetectable in amniotic fluid or cord blood from fetuses whose mothers have quantifiable plasma PGF (Staff *et al.*, 2005).

We postulated that deficiency in fetal PGF would disturb normal cerebrovascular development and initiated comparisons in fetal mice sufficient or genetically-ablated for PGF. Cerebral arterial casts prepared from *Pgf*$^{-/-}$ mice exhibited elongated shape, vascular disorganization and frequently an incomplete Circle of Willis (cW) (Ratsep *et al.*, 2015a). We therefore undertook mouse fetal time course studies of regional brain vascular development to assess when and where PGF contributes to cerebrovascular development.

Materials and Methods

Animals

Male and female B6 mice were purchased from Charles River Canada (St. Constant QU). B6-*Pgf*$^{-/-}$ mice were bred at Queen's University from foundation pairs provided by VIB vzw B-9052 Zwijnaarde, Belgium (Carmeliet *et al.*, 2001). Mice were housed in micro-isolator cages enriched with igloos and nesting materials maintained on an environmental rack and had free access to water and food. Males and pregnant or nursing females were housed individually while non-pregnant females were housed with littermates up to 4 per cage according to our facility's standard procedures. A 12 hour light-12 hour dark cycle was used with an ambient temperature of 23°C. Mice were monitored daily for health and sentinels were assessed regularly to ensure the room that was bioBUBBLE® HEPA air filtered remained free of pathogens. All animal handling was conducted in a laminar flow hood. Females were paired overnight with males. Copulation plug detection was designated embryonic day (E) 0.5. Pregnant females were euthanized by cervical dislocation between E10.5–E18.5, and the fetuses were removed and dissected. For some experiments, neonatal mice (both sexes) at post-natal day (P) 7 or adult non-pregnant female and male mice were euthanized using an injected overdose of sodium pentobarbital or inhaled isoflurane followed by decapitation.

Ethical approval

All procedures were approved by the Queen's University Animal Care Committee (reference number: Croy-2013-006-01) and were consistent with the Canadian Council on Animal Care national standards for ethical animal care and use.

Quantitative real-time PCR for *Pgf, Vegfa, Vegfr1* and *Vegfr2* expression

For quantitative real-time PCR (RT–PCR) analyses, B6 fetal brains (E12.5, 14.5, 16.5, and 18.5 with $n = 5$ fetal brains, each from a different litter at each time point) were dissected using RNAse-free treated forceps and a Heerbrugg microscope (Wild-Leitz, Canada). Three dissected regions, forebrain (FB), midbrain (MB) and hindbrain (HB), were flash frozen in liquid nitrogen. Isolated brain tissues were homogenized and the RNA was purified using RNA binding columns (Norgen Biotek Corp, Thorold, ON, Canada) as per manufacturer's instructions. RNA concentration and purity were determined using a Nanodrop 2000C UV-Vis spectrophotometer (Thermo Scientific, Wilmington, DE, USA) and the extracted RNA was stored at −80°C. The mRNA was reverse transcribed and amplified using the RT^2 First Strand cDNA synthesis kit (Qiagen, Mississauga, ON, Canada). Products were stored at −20°C. Primer assays for genes of interest (*Pgf*—PPMO3669C), (*Vegf*—PPMO03041F), (*Vegfr1/Flt1*—PPMO 3066F), (*Vegfr2/Kdr*—PPMO3057A) obtained from Qiagen (Qiagen, Mississauga, ON, Canada). Plate-based LightCycler 480 reactions (Roche Diagnostics, Laval, QC, Canada) were performed using RT^2 SYBR Green Q-PCR master mix with final reaction volumes of 25 μl. All samples were run in triplicate including Actb as the control. Cycling conditions were denaturation: 95°C; 15 min, amplification: 45 cycles; 95°C for 15 s; 55°C for 30 s; 72°C for 30 s, melting curve: 70–95°C at a rate of 0.1°C/s. Melt curve analyses were performed using LightCycler Software for each gene to verify the specificity of individual PCR products. Relative quantification of each gene was performed using ΔΔCt method and *Actb*.

PGF and VEGF immunolocalization

Heads were collected from B6 fetuses at E12.5, 14.5, 16.5 and 18.5 ($n = 3$ fetal heads from 3 different litters at each time point), fixed in 4% (w/v) paraformaldehyde (PFA) (12 h) and paraffin-embedded. Sections (5 μm) were deparaffinized, rehydrated, blocked in 3% bovine serum albumin and incubated with the anti-mouse polyclonal primary antibodies (0.25 μg/ml anti-PGF (Abcam—ab0542, Toronto, ON, Canada) and 1 μg/ml anti-VEGF (Abcam—ab46162)) for 2 h at room temperature (22°C). Goat anti-rabbit secondary antibodies conjugated to Alexa Fluor 488 (Invitrogen, Ottawa, ON, Canada—A11008) were used for both PGF and VEGF staining in separate sections. At this point, the PE-conjugated anti-CD31 (BD Pharmingen, Mississauga ON—MEC13.3) was added and sections were incubated for 1.5 h at room temperature. Nuclear staining was completed with 4′,6-diamidino-2-phenylindole (DAPI; Life Technologies—D1306, Burlington, ON, Canada). Slides were mounted using Prolong gold anti-fade (Life technologies, Burlington, ON, Canada—9071) and examined using a Zeiss M1 Imager microscope. Multiple fetuses from three different pregnant mice were used per time point.

HB vascularization whole mount immunofluorescent staining

B6 and *Pgf*$^{-/-}$ E10.5 and 11.5 fetuses were fixed in 4% PFA for 2 h. Fetuses from 3 litters were used for each time point and genotype. At E10.5, 21 HBs from 32 B6 fetuses and 18 HBs from 38 *Pgf*$^{-/-}$ fetuses were successfully prepared. Dissected HBs were analyzed whole ($n = 10$ B6 and 9 *Pgf*$^{-/-}$) or in cross-sections ($n = 11$ B6 and 9 *Pgf*$^{-/-}$). At E11.5, 26 HBs from 27 B6 fetuses and 29 HBs from 33 *Pgf*$^{-/-}$ fetuses were successfully prepared. 17 B6 and 21 *Pgf*$^{-/-}$ HBs were imaged whole while 9 B6 and 8 *Pgf*$^{-/-}$ HBs were analyzed as cross-sections. HBs were isolated and the vasculature stained using the protocol of Fantin *et al.* (2013). Briefly, isolated HBs were blocked using 0.1% Triton-X (BioShop, Burlington, ON, Canada—TRX506) and 10% normal goat serum (NGS) (Sigma, Oakville, ON, Canada—G9023) in PBS. After washing, HBs were incubated overnight with 40 μg/ml Tetramethylrhodamine (TRITC)-conjugated isolectin B4 (IB4; Sigma, Oakville, ON, Canada—L5264), an endothelial cell marker. The ventricular plexus was imaged using a Zeiss M1 Imager fluorescence microscope (Zeiss; Toronto, ON, Canada) equipped with an AxioCam and Axiovision 4.8 software. Cross sections of the HB were imaged with a Quorum Wave FX Spinning Disc confocal microscope (Quorum; Guelph, ON, Canada). Three dimensional confocal images were reconstructed with MetaMorph software (Molecular Devices; Sunnyvale, California, USA). Analysis was performed using ImageJ by a single blinded reviewer. HBs were processed in batches and measurements from each HB were not linked to fetal size or sex.

Circle of Willis whole mount immunofluorescent staining

Formation and connectivity of cW were evaluated in B6 and *Pgf*$^{-/-}$ E14.5 and P7 mice. Fetal studies used all pups from three litters for each genotype. Neonatal studies used at least three pups from each of three litters per genotype. Males and females were studied at both stages. Fetuses were fixed in 4% PFA overnight at 4°C before dissection. P7 mice were anesthetized using pentobarbital 50 mg/kg intraperitoneally and perfused via the left ventricle with 1 ml 4% PFA after which the heads were immersion-fixed in 4% PFA overnight. Skulls were removed for visualization of the anterior cW. After blocking in PBS with 0.1% Triton-X and 10% NGS, brains were incubated with a 10 μg/ml IB4 solution. After washing, the anterior cW was visualized using a Zeiss M1 Imager microscope. The posterior cerebral and communicating arteries were not analyzed due to technical difficulties in dissecting posterior brain. Image analysis was performed using ImageJ. Fetal and neonatal body and brain dimensions as well as cW vessel diameters, connectivity and vessel numbers were quantified by a single blinded reviewer.

Ink perfusion and circle of Willis imaging

Mice ($n = 4$ male and 3 female B6 and $n = 3$ male and 4 female *Pgf*$^{-/-}$) were anesthetized intraperitoneally with 50 mg/kg sodium pentobarbital. Mice were perfused with 2 ml PBS through the left ventricle followed by 2 ml Pelikan black ink (Wallack's Art Supplies, Kingston, ON). The brains were isolated and images of the cW were obtained with a Zeiss Lumar.V12 stereo microscope (Carl Zeiss, Oberkochen, Germany) with Motic Images Plus 2.0 (Motic, Hong Kong, China). Measurements of cW dimensions, vessel length, angles and diameters as well as number of vessels were completed using ImageJ by a blinded reviewer.

Left common carotid artery ligation ischemic infarct assay

Adult B6 and *Pgf*$^{-/-}$ mice were anesthetized with isoflurane (Pharmaceutical Partners of Canada, Richmond Hill, ON, Canada) in 20%:80% O_2:N_2 and maintained at 36 ± 0.5°C using a rectal probe and heating pad. Cerebral blood flow was measured with laser Doppler flowmetry (Perimed, Periflux System 5010, North Royalton, OH, USA). The left common carotid artery (LCCA) was occluded using a 6–0 silk suture for 30 min then the anesthetized mice were decapitated ($n = 14$ B6 and 15 *Pgf*$^{-/-}$ male and female mice). In a subset of the mice, ($n = 6$ B6 and 9 *Pgf*$^{-/-}$) cerebral blood flow was measured before LCCA ligation and throughout the experiment. The percent of initial blood flow remaining after LCCA ligation was calculated and compared. Brains were rapidly excised under a drip of ice-cold phosphate-buffered saline (PBS), cut into 1 mm thick coronal sections using an adult mouse brain matrix (Zivic Instruments, #BSMAS001-1, Pittsburgh, PA, USA) and stained with 0.5% 2,3,5-triphenyltetrazolium chloride in PBS (TTC; Sigma Aldrich, #T8877, Mississauga, ON, Canada). Images of these tissues were captured using a Zeiss Lumar.V12 stereo microscope (Carl Zeiss, Oberkochen, Germany) with Motic Images Plus 2.0 (Motic, Hong Kong, China). The presence of an ischemic tissue was determined by

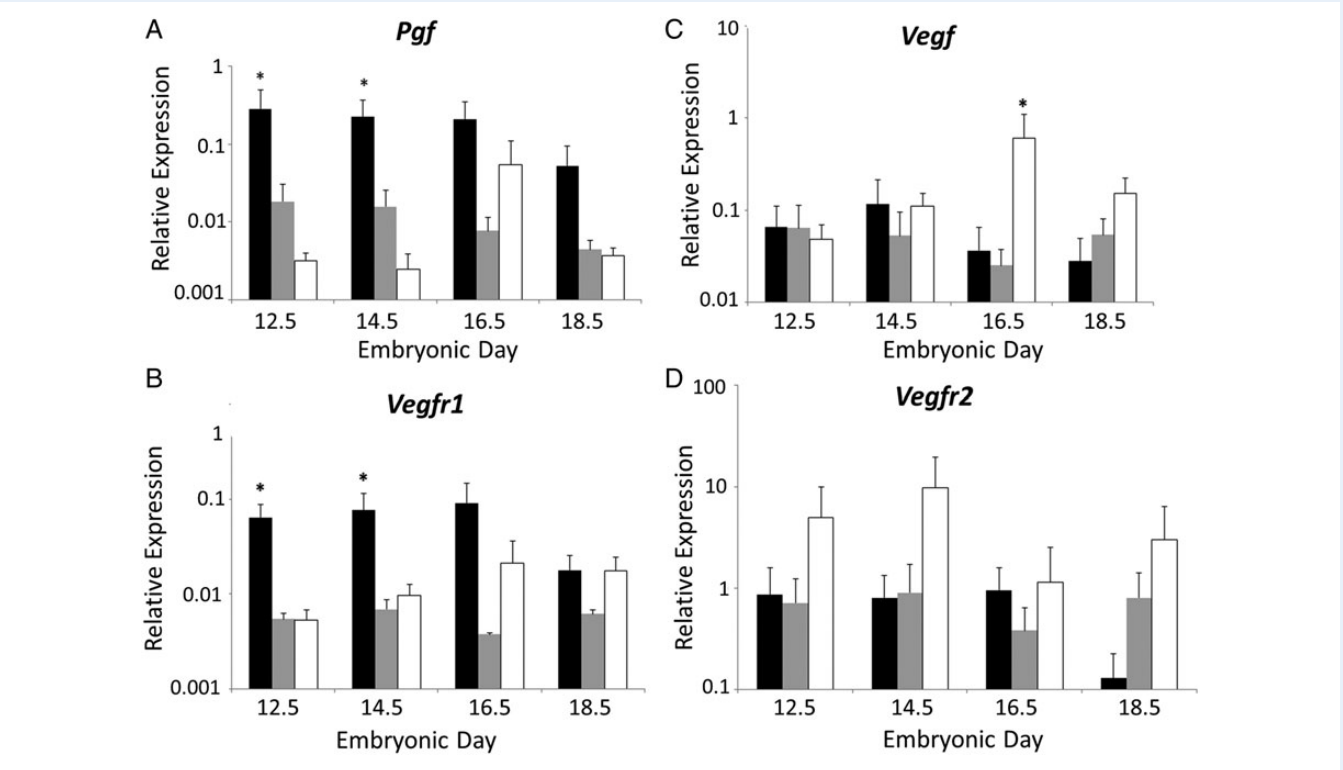

Figure 1 Relative gene expression in B6 fetal brains. Quantitative PCR data are shown for relative expression of mRNA for *Pgf* (**A**), *Vegfr1* (**B**), *Vegf* (**C**) and *Vegfr2* (**D**) by fetal brain regions. The brains were dissected into forebrain (FB) (black bars), midbrain (MB) (gray bars) and hindbrain (HB) (white bars) at embryonic day (E) 12.5, 14.5, 16.5 and 18.5. Results were considered significant when $P < 0.05$ (*) or $P < 0.02$ (**) for comparisons between the brain areas and $P < 0.05$ ($^{\#}$) or $P < 0.02$ ($^{\#\#}$) for comparisons between the gestational times. β-actin was used as the reference gene.

a blinded reviewer and the size was measured using ImageJ. Size of the ischemic area was corrected for edema using the ratio of the size of the unaffected to the affected hemispheres.

Statistical analysis

The gene expression data obtained by qPCR was analyzed with an ANOVA for repeated measures using the PROC GLM procedure of the Statistical Analysis System (SAS 9.0; Toronto, Ontario, Canada). Effects of brain region, embryonic day and interactions were included in the model. Correlations between genes were assessed using the PROC CORR procedure of SAS. Two-way analysis of variance (ANOVA) and Bonferroni-corrected post-tests were used to test the statistical significance of differences in HB vascularization and cW development with one mouse or one fetus as a unit of analysis (Graphpad Prism; San Diego, California, USA). An unpaired *t*-test was used to analyze the difference between genotypes in cerebral blood flow after LCCA ligation.

Results

Pgf/*Vegf* and *Vegfr1*/*Vegfr2* expression time courses in B6 fetal brain

Relative abundance of transcripts for *Pgf*, *Vegf*, *Vegfr1* and *Vegfr2* was measured in fetal FB, MB and HB homogenates at mid to late gestation (Fig. 1). Brain regions and gestational times were compared independently. Relative *Pgf* expression was significantly higher in FB than MB or HB at E12.5 ($P = 0.001$) and at E14.5 ($P = 0.04$). At E16.5, relative *Pgf* expression was significantly greater when FB was compared with MB ($P < 0.05$) but not with HB. By E18.5, no statistically significant differences were present between relative *Pgf* expression in FB, MB and HB. Relative *Pgf* expression in MB did not change over gestation. Relative *Vegfr1* expression was statistically significantly higher in FB at E12.5 ($P = 0.011$) and E14.5 ($P = 0.011$) compared with either MB or HB. At E16.5, FB had greater relative *Vegfr1* expression than MB but not HB. Relative *Vegfr1* expression in MB and HB did not change throughout the gestational study interval and was not significantly different when compared with other brain areas. Relative expression of *Vegf* was also stable across gestation, except for a peak in expression in E16.5 HB. This was the only time point at which relative *Vegf* expression was significantly higher in HB than in FB or MB ($P = 0.001$). There were no significant changes in relative expression of *Vegfr2* at any of the analyzed gestational times or between the FB, MB and HB. These data suggest dynamically regulated, anatomically specific importance for PGF in midgestational development of forebrain vessels.

Immunolocalization of PGF and VEGF in B6 fetal brain

To confirm that the pathways that promote angiogenesis in developing brain include signaling via PGF protein, immunofluorescent staining was undertaken for PGF/CD31/DAPI and VEGF/CD31/DAPI on transverse sections of fetal B6 brains. At E12.5 (Fig. 2A), PGF expression was predominant in FB, most notably in the diencephalon. Expression

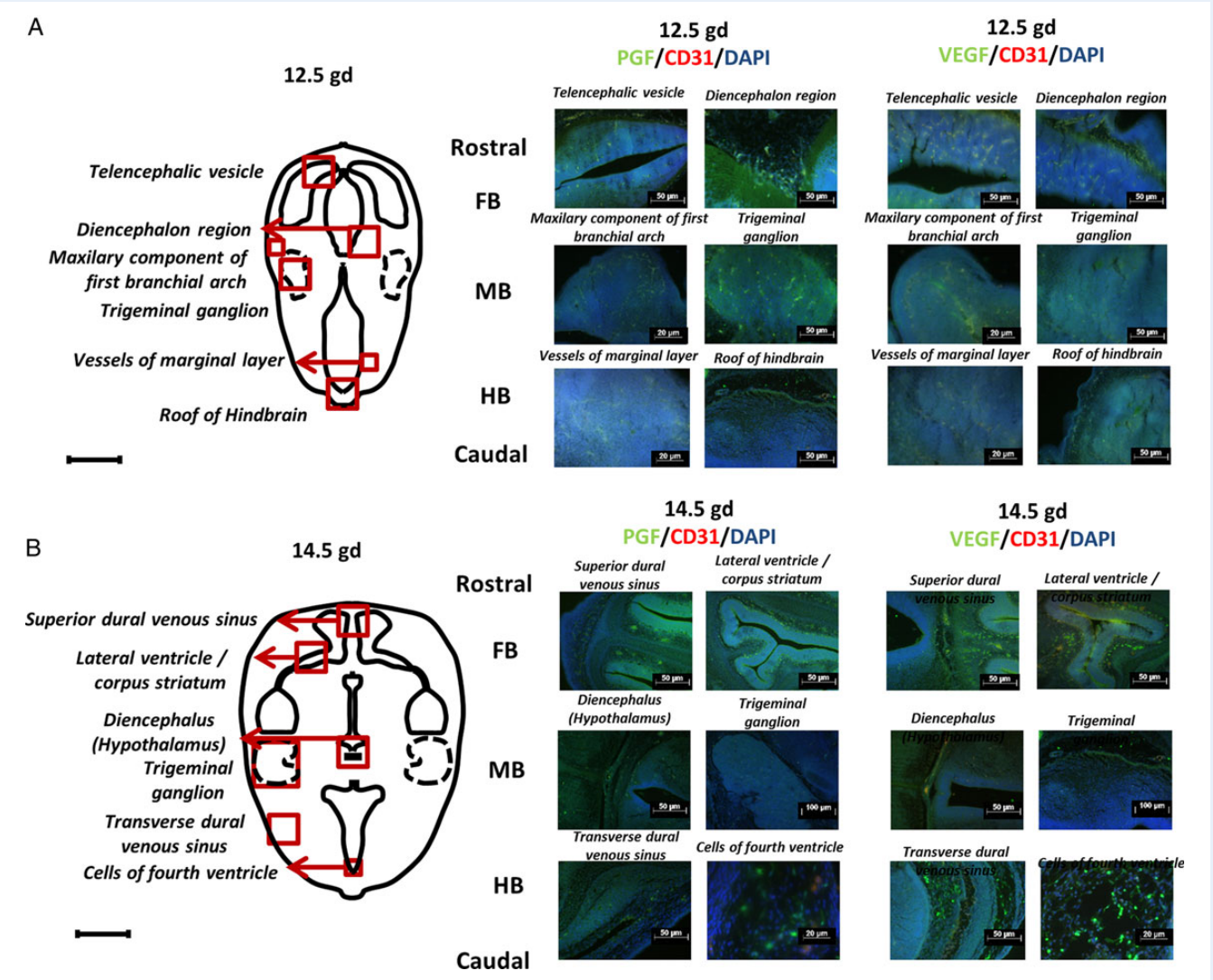

Figure 2 Immunolocalization of placental growth factor (PGF) and vascular endothelial growth factor (VEGF) in embryonic day (E) 12.5 and E14.5 B6 fetal brains. Images depict immunofluorescent staining of PGF (green), VEGF (green) and CD31 (red) and nuclear staining by 4′,6-diamidino-2-phenylindole (DAPI) (blue) in fetal brain at E12.5 (**A**) and E14.5 (**B**). Two areas from each region (Fore-, mid- and hind-brain; FB, MB and HB) were chosen. The schematic drawings locate the following structures at E12.5 (telencephalic vesicle, diencephalon region, maxillary component of first branchial arch, trigeminal ganglion, vessels of marginal layer, roof of HB) and at E14.5 (superior dural venous sinus, lateral ventricle/corpus striatum, diencephalon (hypothalamus), trigeminal ganglion, transverse dural venous sinus, cells of fourth ventricle).

was seen in both nervous and vascular tissue. In MB, PGF and VEGF appeared to be expressed at similar levels by fluorescence quenching time measurements in the maxillary component of the first branchial arch and trigeminal ganglion. In HB, VEGF was more highly expressed than PGF in the roof but not in vessels of the marginal layer. In the latter images, the anti-CD31 fluorescent staining was overwhelmed by high endothelial cell expression of PGF and VEGF.

At E14.5 (Fig. 2B), PGF and VEGF expression appeared unchanged in the superior dural venous sinus and lateral ventricle/corpus striatum of the FB. Equivalent expression of PGF and VEGF was also observed in the diencephalon (hypothalamus) and trigeminal ganglion. In HB areas, VEGF localization was predominant in the transverse dural venous sinus and especially in cells of fourth ventricle.

At E16.5 (Fig. 3A), FB had greater expression of PGF than VEGF. This difference was stronger in the wall of telencephalon than in the lateral ventricles. In E16.5 MB, VEGF expression was high in the transverse dural venous sinus while PGF expression was strong in the mesencephalic vesicle. In the selected HB areas, primitive cerebellum and its vessels showed the highest VEGF expression.

At E18.5 (Fig. 3B), expression of PGF and VEGF was localized to vessels of the white matter and superior horn of lateral ventricle as well as to vessels in the hippocampus and transverse dural venous sinus. Patterns of PGF and VEGF expression were similar in FB and MB. In contrast, in HB, the posterior part of the cerebellum had greater VEGF localization while the posterior semi-circular canal exhibited comparable levels of PGF and VEGF staining.

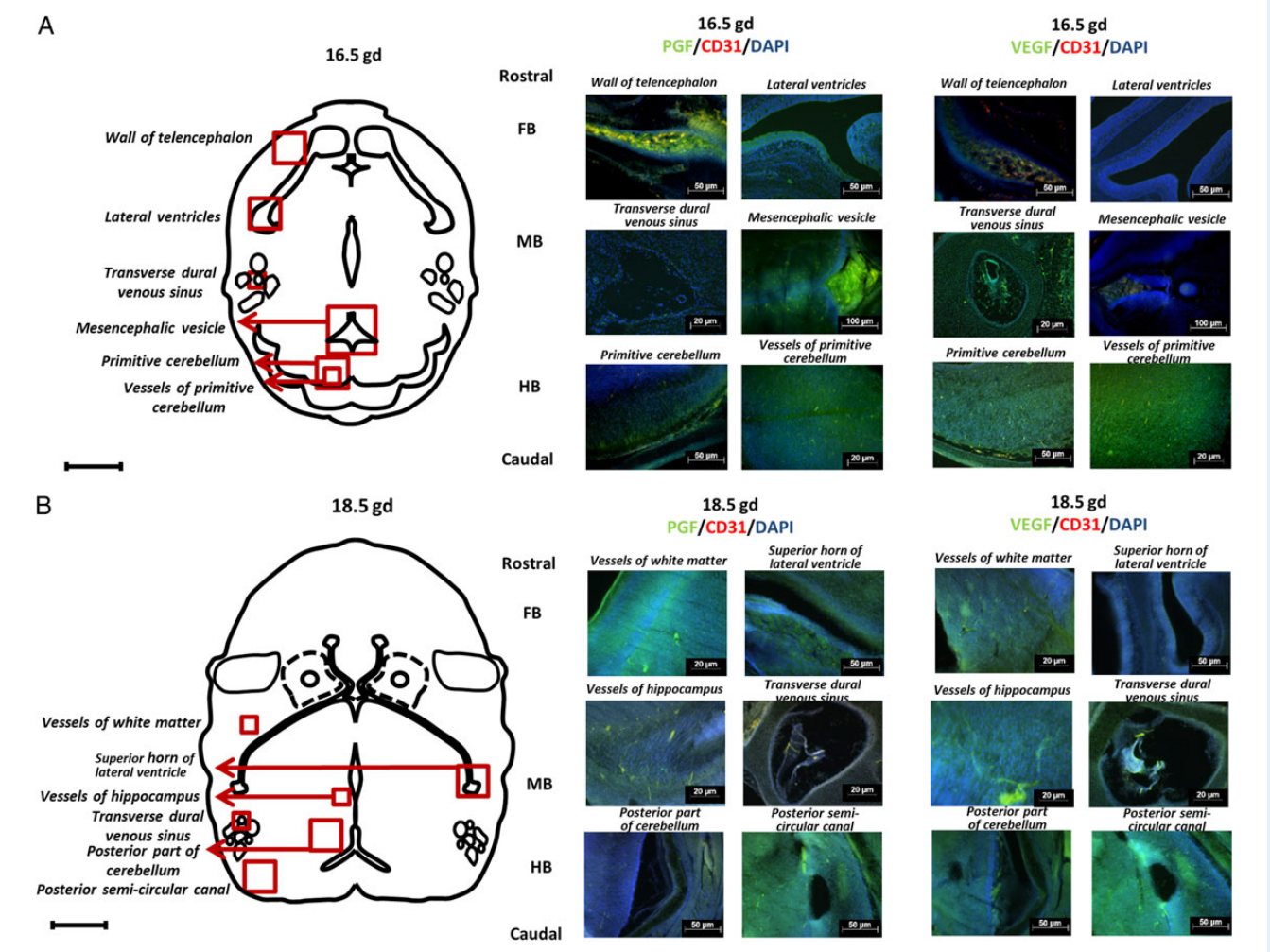

Figure 3 Immunolocalization of placental growth factor (PGF) and vascular endothelial growth factor (VEGF) in embryonic day (E) 16.5 and 18.5 B6 fetal brains. Images depict immunofluorescence staining of PGF (green), VEGF (green) and CD31 (red) and nuclear staining by 4′,6-diamidino-2-phenylindole DAPI (blue) in fetal brain at E16.5 (**A**) and E18.5 (**B**). Two areas from each region (Fore-, mid- and hind-brain; FB, MB and HB) were chosen. The schematic drawings show the location of the wall of telencephalon, lateral ventricles, transverse dural venous sinus, mesencephalic vesicle, primitive cerebellum, and vessels of primitive cerebellum at E16.5 as well as the vessels of white mater, superior horn of lateral ventricle, vessels of hippocampus, transverse dural venous sinus, posterior part of cerebellum, and posterior semi-circular canal at E18.5.

HB vascularization in E10.5 and 11.5 *Pgf*$^{-/-}$ and B6 mice

Mouse fetal HB vascularization is usually assessed at E10.5. However, we observed that *Pgf*$^{-/-}$ mice were smaller than B6 at E10.5 and therefore made comparisons at E10.5 and E11.5 (Fig. 4A and B). At both times, *Pgf*$^{-/-}$ fetuses were growth-restricted compared with B6 with significantly shorter head lengths ($P = 0.006$) at E10.5 and significantly less width ($P = 0.001$) at E11.5 (Supplementary Fig. S1). The majority of *Pgf*$^{-/-}$ fetuses had no developmental delays as assessed by Theiler staging (data not shown) (Kaufman, 1992). Two E11.5 *Pgf*$^{-/-}$ fetuses at lower Theiler stages were excluded from analysis. Vessels in the E10.5 *Pgf*$^{-/-}$ HB ventricular plexus were significantly thinner than in B6 ($P = 0.0008$, Fig. 4C) and *Pgf*$^{-/-}$ HB vessel junctions per area were significantly greater ($P < 0.001$, Fig. 4D). E10.5 *Pgf*$^{-/-}$ HB cross-sections revealed narrower sprout diameters ($P = 0.022$, Fig. 4E) than B6, further suggesting that HB vascularization is impaired at E10.5 by PGF deficiency. By E11.5, differences in CNS development were more apparent and HB thickness was significantly lower ($P = 0.0002$, Fig. 4F) in *Pgf*$^{-/-}$ fetuses despite normalization of the HB vasculature with respect to vessel diameter, number of junctions and sprout diameter. Thus, the transient delay in vascular development linked with PGF deficiency was sufficient to impact CNS structural development.

Circle of Willis in E14.5, P7 and adult *Pgf*$^{-/-}$ and B6 mice

The anterior cW was visualized and imaged in E14.5 and P7 *Pgf*$^{-/-}$ and B6 brains (Fig. 5A and B). Although body weights were similar for both genotypes, P7 *Pgf*$^{-/-}$ brains were smaller than B6 ($P < 0.001$, Supplementary Fig. S1). Analyses of arterial diameters and the number of vessels revealed defects in the *Pgf*$^{-/-}$ cW. In normal B6 brains, the anterior cerebral arteries (ACA) were different in size with one ACA on average 80% the width of the other. However, in *Pgf*$^{-/-}$ E14.5 and P7 brains, this difference in

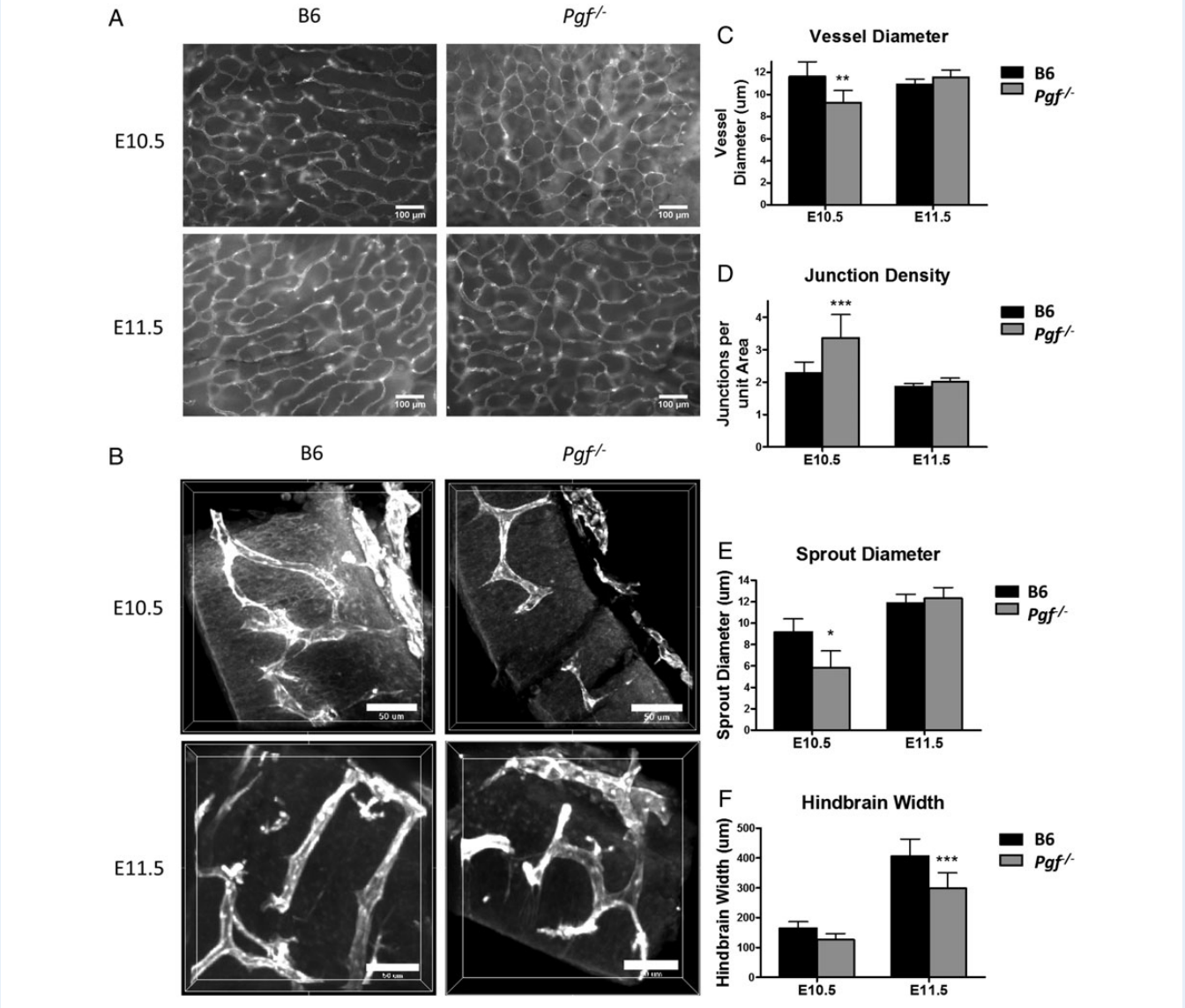

Figure 4 Whole mount vascular staining of hindbrain (HB) at embryonic day (E) 10.5 and 11.5. HB vascularization was compared between B6 and $Pgf^{-/-}$ fetuses at E10.5 and 11.5 by examining the isolectin B4 (IB4) stained (white) ventricular plexus (**A**) and sprouting in transverse sections of the hindbrain (**B**). In the ventricular plexus, vessel diameter was thinner in the $Pgf^{-/-}$ HB vasculature at E10.5 (**C**). Conversely, the number of junctions per area was significantly greater in the E10.5 $Pgf^{-/-}$ HB vascular plexus (**D**). Confocal imaging of the HB cross-sections revealed smaller sprout diameter (**E**) and reduced HB thickness (**F**) in the $Pgf^{-/-}$ HBs. Means with 95% confidence intervals are shown with $P < 0.05$, $P < 0.01$, and $P < 0.001$ represented by *, **, and *** respectively.

arterial diameter was exaggerated, suggesting unilateral hypoplasia of one ACA. The diameter of the thinner ACA was less in $Pgf^{-/-}$ brains than in B6 ($P < 0.0001$ at P7, Fig. 5C) while the diameter of the wider ACA was similar between $Pgf^{-/-}$ and B6 brains. This difference was reflected in the decreased ratio of the two ACA diameters in $Pgf^{-/-}$ mice ($P = 0.012$ at E14.5; Fig. 5D). However, when ink perfusion was used to compare the cW in adult mice (Fig. 6A) there was no significant difference between genotypes for either the thicker or thinner ACA diameter (data not shown).

The total number of vessels in the anterior cW is decreased by absence of PGF (Fig. 5E and F). The anterior communicating artery (AComA) was absent in a significant proportion of E14.5 $Pgf^{-/-}$ brains; 45.5% had no AComAs, 50% had one AComA and only 4.5% had more than one AComA. In B6, 58.3% and 41.7% of fetuses had one or more than one AComA respectively. This reduction in the presence of AComAs is reflected in a significantly decreased average number in $Pgf^{-/-}$ mice ($P = 0.0005$; Fig. 5E). Similarly, in adulthood, the average number of communicating vessels was significantly less in $Pgf^{-/-}$ mice, particularly in the female mice ($P < 0.05$, Fig. 6B).

The number of collateral vessels present in the anterior cW also differed in $Pgf^{-/-}$ mice. At E14.5, 50% of B6 fetuses had an extra vessel, 25% had more than one extra vessel and only 25% did not have an extra vessel while in $Pgf^{-/-}$ fetuses, 86.4% had no extra vessels, 13.6% had one extra vessel and none had more than one extra vessel. The average number of collateral vessels was significantly less in $Pgf^{-/-}$ mice as a result ($P < 0.001$;

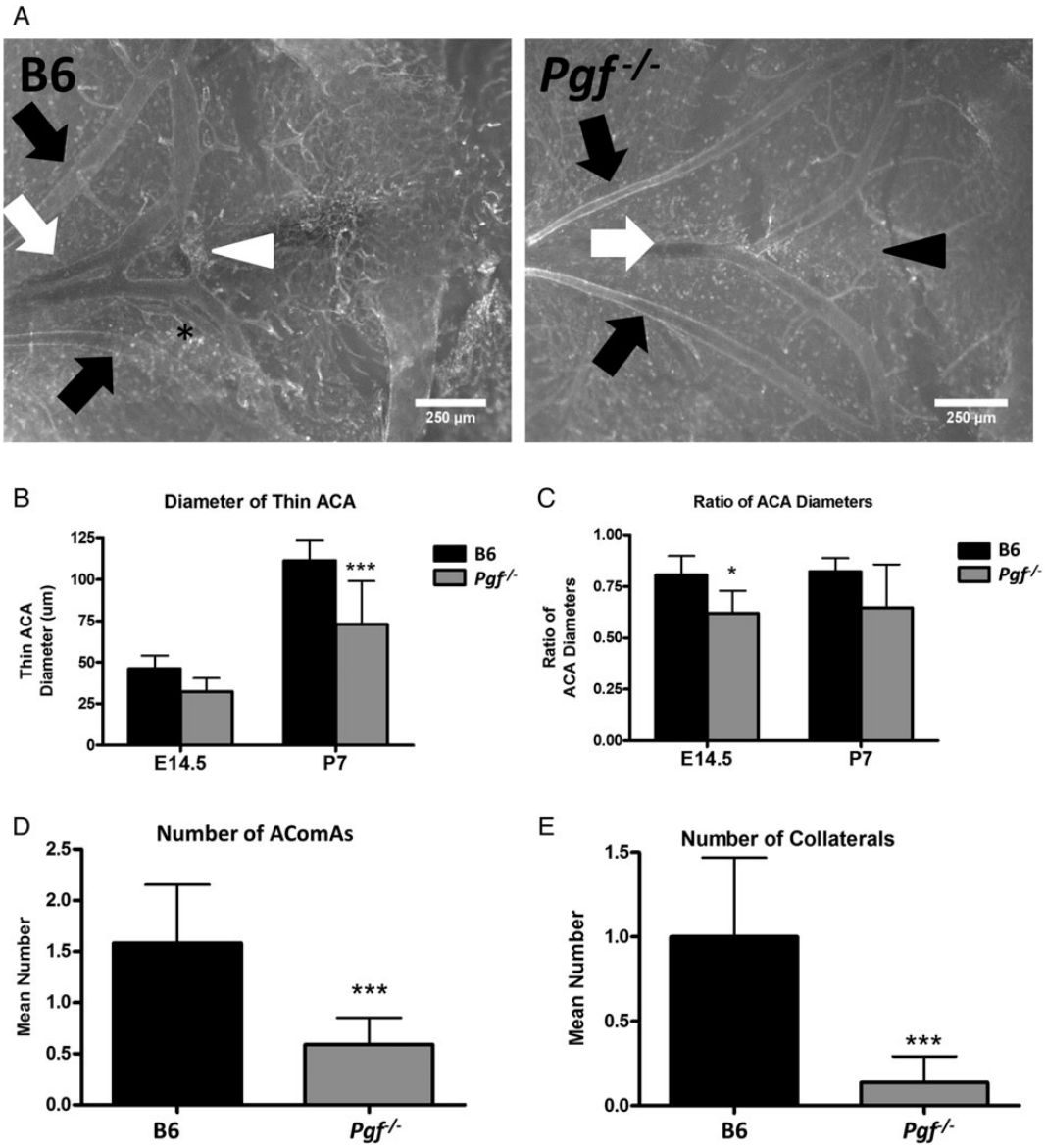

Figure 5 Whole mount vascular staining of circle of Willis (cW) at embryonic day (E) 14.5 and post-natal day (P) 7. Whole mount immunofluorescence with isolectin B4 (IB4; white) provided visualization of the anterior cerebral arteries (ACAs: white arrows), olfactory arteries (black arrows) and the anterior communicating artery (AComA; white arrowhead) in B6 and $Pgf^{-/-}$ brains at E14.5 (**A**) and P7 (not shown). In many B6 brains, an extra vessel along the ACA was present (asterisk) while in some $Pgf^{-/-}$ brains, the AComA was absent (black arrowhead). Significant changes in the $Pgf^{-/-}$ cW included a narrower diameter of one ACA (**B**) but not both ACAs, resulting in a decreased ratio of the ACA diameters (**C**). The number of vessels present in the anterior cW of $Pgf^{-/-}$ mice was fewer than in B6 mice. The mean number of AComAs in the $Pgf^{-/-}$ cW at E14.5 was fewer than in B6 (**D**). Similarly, at E14.5, the mean number of collateral vessels in the $Pgf^{-/-}$cW was reduced (**E**). Means with 95% confidence intervals are shown with $P < 0.05$, $P < 0.01$, and $P < 0.001$ represented by *, **, and *** respectively.

Fig. 5F). However, there was no statistically significant difference in the number of collateral vessels in the adult $Pgf^{-/-}$ circle of Willis (Fig. 6C). Overall, while the anterior cW is still complete in $Pgf^{-/-}$ mice, its reduced number of vessels suggests that $Pgf^{-/-}$ mice may be vulnerable to cerebrovascular insults due to collateral vessel deficiencies.

Left common carotid artery ligation (LCCA)

LCCA was conducted on male and female B6 and $Pgf^{-/-}$ mice to assess susceptibility to ischemia. During the surgeries, it was noted that some $Pgf^{-/-}$ animals had abnormal vascular anatomy including absence, duplication or hypoplasia of the internal carotid artery (ICA).

In B6 mice, no infarct was identified after 30 min ligation (Fig. 7A). However, in two $Pgf^{-/-}$ females (out of 15 $Pgf^{-/-}$ mice total), infarcts were identified with volumes of 45.91 and 46.77 mm^3 respectively (Fig. 7B). The percentage of cerebral blood flow remaining after LCCA ligation was also significantly less in $Pgf^{-/-}$ mice ($P = 0.0102$, Fig. 7D). Therefore, increased $Pgf^{-/-}$ susceptibility to an ischemic episode may be associated with structural arterial variations, particularly in the ICA.

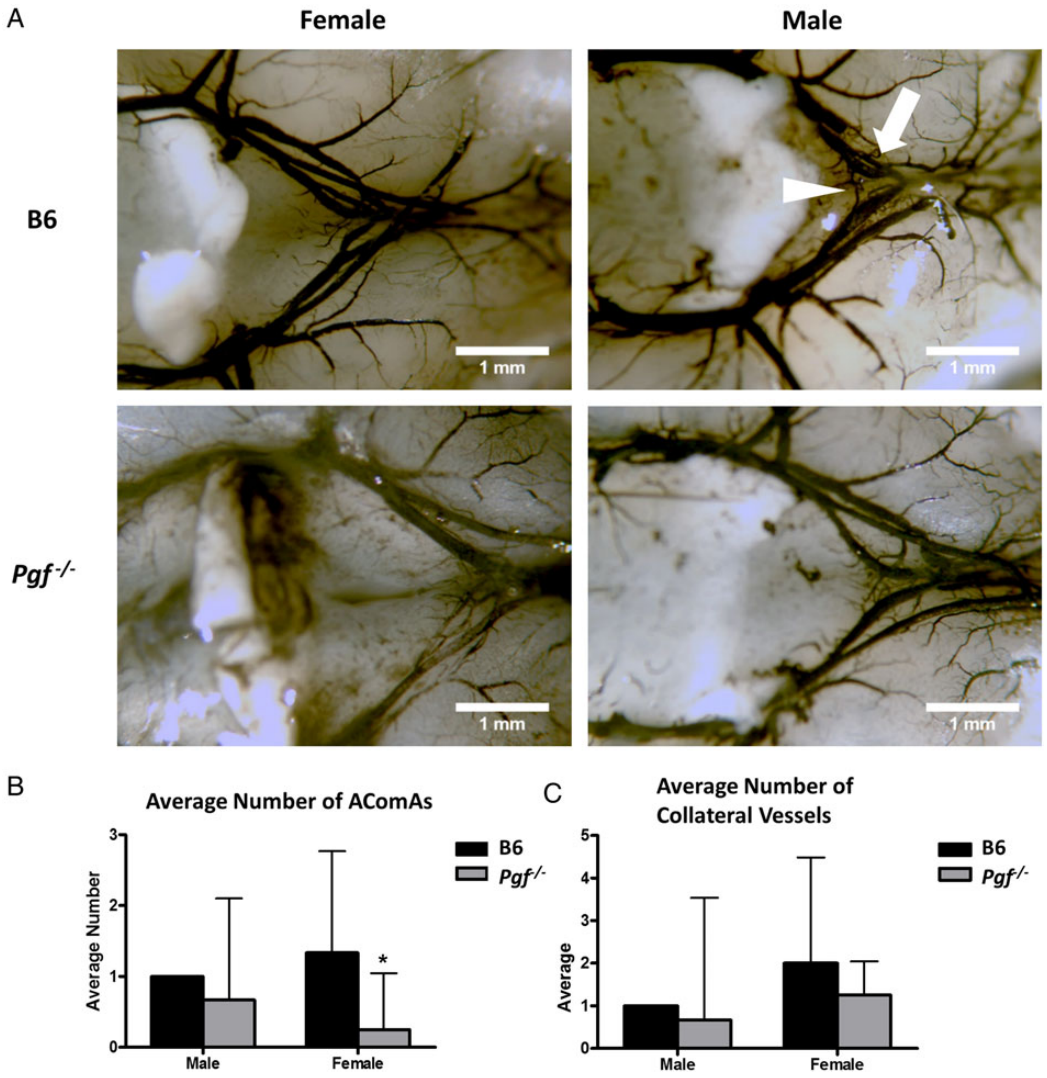

Figure 6 Ink perfusion and imaging of the adult circle of Willis. The circle of Willis was imaged in adult male and female B6 and $Pgf^{-/-}$ mice (**A**). The average number of anterior communicating arteries (AComAs) (arrowhead) was decreased in female $Pgf^{-/-}$ mice (**B**). There was no significant difference in the number of anterior collateral vessels on the anterior cerebral arteries (arrow) in either male or female $Pgf^{-/-}$ mice (**C**). Means with 95% confidence intervals are shown with $P < 0.05$ represented by *.

Discussion

PGF deficiency in mice deviates cerebrovascular development and impacts vessels of varying sizes. HB vascularization was delayed in $Pgf^{-/-}$ mice and this was accompanied by a narrower HB, a difference that persisted following normalization of the vascular bed at E11.5. Based on relative expression analyses, it appears that VEGF is more important for HB vascularization than PGF. VEGF compensation, driven by hypoxia, may explain the normalization of HB vessels at E11.5. However, reports of increased systolic arterial pressure in $Pgf^{-/-}$ mice (Steenkiste *et al.*, 2011; Aasa *et al.*, 2015) suggest that vascular differences persist into adulthood.

PGF deficiency permanently affected the developing cW. Murine internal carotid, cerebral and basilar arteries form prior to E11.5 from the transient aortic arches (Hiruma and Nakajima, 2002). The anterior communicating artery (AComA) completes the cW between E11.5–15.5 (Yang *et al.*, 2013). Although the anterior cW was complete in $Pgf^{-/-}$ mice, defects predictive of decreased blood flow were identified. Incomplete cW development was previously reported in mice deficient in vascular smooth muscle cell Notch signaling (Proweller *et al.*, 2007; Yang *et al.*, 2013). In these animals, AComA narrowing was found despite normal abundance of VEGFA protein (Yang *et al.*, 2013). ACA unilateral hypoplasia with fewer communicating and collateral arteries was observed in $Pgf^{-/-}$ mice. These changes may have limited impact on brain health under normal conditions but would increase sensitivity to ischemia when blood flow is obstructed. This hypothesis is supported by the infarcts observed in two $Pgf^{-/-}$ females after LCCA occlusion and probably explains why radiotelemetry experiments were previously unsuccessful in 80% of adult $Pgf^{-/-}$ males and females (Ratsep *et al.*, 2015a). In our experiments, LCCA occlusion was maintained for only

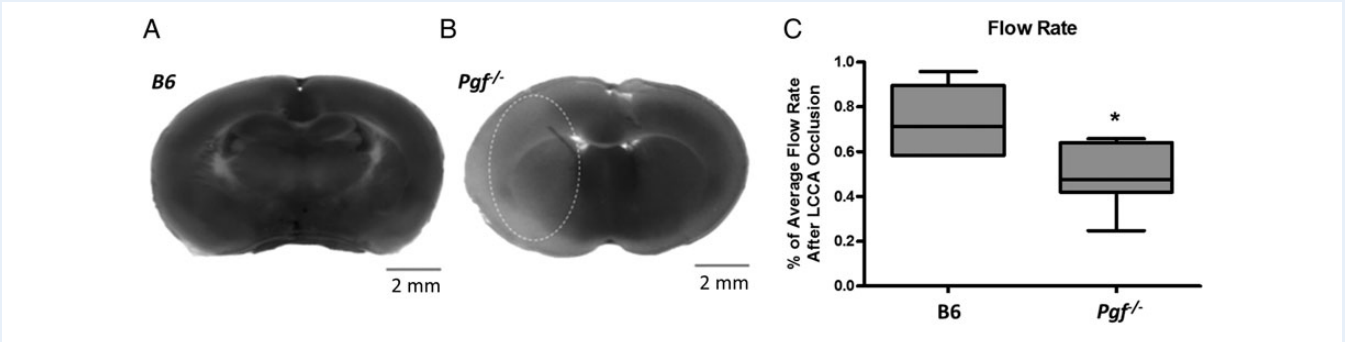

Figure 7 Infarct size and blood flow after left common carotid artery (LCCA) occlusion. Staining revealed no apparent infarct in B6 brain slices (**A**) but infarcted tissue (pale area encircled) in 2 female *Pgf*$^{-/-}$ mice (**B**). The percentage of cerebral blood flow remaining after LCCA was significantly decreased in the *Pgf*$^{-/-}$ mice (**C**). * represents $P < 0.05$.

30 min, a relatively mild insult. Although only two animals developed infarcts, the number may have been higher with a longer protocol. In fact, significantly greater decreases in cerebral blood flow were identified in the *Pgf*$^{-/-}$ mice after LCCA occlusion compared with B6 mice even without appearance of an infarct.

Although both animals experiencing infarcts were female and AComA differences were identified in adult female *Pgf*$^{-/-}$ brains, too few ischemic events occurred to conclude there is a sex difference. However, sexually dimorphic gene expression has been reported in preimplantation mouse embryos suggesting that developing offspring will respond differently to stresses (Lowe *et al.*, 2015). In preeclamptic pregnancies, the inflammatory, angiogenic and apoptotic responses differ by fetal sex (Muralimanoharan *et al.*, 2013). Further, sexually dimorphic effects on placental and brain function after *in utero* stress or alcohol exposure have been reported (Lan *et al.*, 2015). The brain has been identified as sexually dimorphic both structurally (Goldstein *et al.*, 2001; Gong *et al.*, 2011; Yan *et al.*, 2011) and vascularly (Tontisirin *et al.*, 2007; Krause *et al.*, 2011). Therefore, we suspect that PGF deficiency and *in utero* experience of PE will impact male and female brains differently. Although PGF is known to be important for collaterogenesis in wound healing and ischemia (Dewerchin and Carmeliet, 2012), it is not yet possible to assign the cerebrovascular phenotype we observed directly to a PGF deficiency, rather it reflects disturbances within angiogenic pathways. Notch signaling is intricately entwined with PGF and VEGF signaling with effects upstream and downstream of *Vegfr1*. Delta-like ligand 4/NOTCH signaling increases expression of *Vegfr1* while decreasing expression of *Pgf* in endothelial cells (Harrington *et al.*, 2008). Conversely, inhibition of the NOTCH pathway rescues branching defects in *Vegfr1*$^{-/-}$ endothelial cells (Chappell *et al.*, 2013).

In humans, the cW is formed between days 40 and 55 of pregnancy (Van Overbeeke *et al.*, 1991; Degani, 2009). The human cW is a highly variable structure, particularly in its posterior components which are incomplete in 22% of normal individuals (Ryan *et al.*, 2013). Defects in the cerebral vasculature following gestational PGF deficiency could explain the higher incidence of stroke in offspring of preeclamptic pregnancies. Although PE occurs acutely in women after week 20 of gestation, low PGF levels in maternal plasma are present by the first trimester in many women who progress to PE (Vatten *et al.*, 2007; Romero *et al.*, 2008). Thus, the timeframes for suboptimal placental PGF production and cW development overlap. In our knockout model, PGF expression is absent in all tissues, including the placenta and the brain. While the placenta has not been excluded as the source of PGF that regulates cerebral vascular development and other studies implicate placental hormones and neurotransmitters in offspring brain development (Bonnin *et al.*, 2011; Penn *et al.*, 2014), we have now documented localized and dynamic expression of PGF in developing brain tissue.

This study is the first to describe PGF levels in the developing mouse brain. Previous reports address PGF expression in human brain tumors (Donnini *et al.*, 1999) and after ischemic injury in cerebral vessels, neurons and astrocytes in mice and rats (Beck *et al.*, 2002; Du *et al.*, 2010). In adult human brain, PGF is expressed in neurons but not glial cells (Xu *et al.*, 2012a). PGF was increased in human cerebrospinal fluid after seizures (Xu *et al.*, 2012b) suggesting PGF has an important neuroprotective, homeostatic role. Neuroprotection could be due to improved neoangiogenesis, (Gaál *et al.*, 2013) to direct effects on neural cells or to combined effects. Since PGF affects both neuronal and vascular structures, our study cannot determine the temporality of deficits in collateral vessels and brain growth in *Pgf*$^{-/-}$ mice. Impaired brain development may result from vascular deficiencies caused by the lack of PGF. Conversely, impaired brain development caused directly by the lack of PGF may lead to impaired vascularization. PGF is known to act directly on endothelial cells, but also has roles in mural cell and macrophage recruitment (Dewerchin and Carmeliet, 2012). Deficient mural cell recruitment may also impair arteriogenesis (Gaál *et al.*, 2013). Similarly, macrophages have important roles in the formation of anastomoses and are important for collateral vessel formation (Pipp *et al.*, 2003; Duelsner *et al.*, 2012). Therefore, absence of PGF during development may lead to reduced angiogenesis and arteriogenesis through several different pathways.

Developmental analysis of the different brain regions is important to understand disorders that present in childhood or adult life. In this study, we chose regions that mature into significant structures including the cerebral cortex, thalamus, cerebellum, and venous plexus. PGF and VEGF and their receptors were expressed by both cerebral tissue and by vessels in the FB, MB and HB at all gestational time points although the strength of expression varied between brain regions and developmental stages. Based on expression strength, PGF should have the greatest influence on the FB, the primordium of brain regions associated post-natally with executive and cognitive functions, while VEGF was more predominant in the HB and would have greater influence on areas related to the future fourth ventricle and cerebellum. Smaller head circumference

at birth (Kajantie *et al.*, 2009), cognitive impairments, and mood disorders at advanced ages are reported in offspring of preeclamptic pregnancies compared with controls matched for current and gestational-ages (Tuovinen *et al.*, 2010, 2012, 2013). Recent pilot studies of 10 children age 7–10 years, who experienced PE gestations compared with sex, gestation-length and age-matched controls, demonstrated cerebral vascular and anatomic differences that were accompanied by PGF deficiency in maternal term plasma (Ratsep *et al.*, 2015b). This literature and the findings reported here regarding anomalous cerebral vascularization in $Pgf^{-/-}$ mice and its impact on early brain tissue structure suggest that cerebral angiograms and further anatomic magnetic resonance imaging scans of offspring of preeclamptic pregnancies may provide a new dimension in understanding lifelong cerebral consequences for offspring from PE gestations.

Conclusion

We characterized the expression of PGF in the developing mouse brain from mid to late gestation, identified multiple cerebral vascular defects induced by PGF deficiency and provided evidence that disturbed cerebral vascularization can precede an alteration in CNS structure and blood flow. While PGF is already described as a therapeutic target in neurologic diseases, our results indicate that normal levels of PGF during development have critical importance. Further, fetal PGF deficiency would increase susceptibility to stroke due to differentiation of relatively narrow cerebral vessels and failure to develop a normal frequency of collateral vessels.

Supplementary data

Supplementary data are available at http://molehr.oxfordjournals.org/.

Acknowledgements

The authors are grateful to Dr Rami Kridli (University of Guelph) for support with statistical analyses, Ms Nicole Ventura (Queen's University) for assistance with PCR studies, Dr David Andrew (Queen's University) for the use of his vibratome and Dr Chandrakant Tayade (Queen's University) for access to his laboratory facilities and technical instruction.

Authors' roles

R.L.L., V.R.K., A.J. and B.A.C. designed the studies. R.L.L. performed the PCR and immunofluorescence analysis of PGF expression in developing mouse brain. K.K. and M.B. assisted with the PCR experiments and their analyses. V.R.K. performed the whole mount comparisons of HB vasculature and the circle of Willis. N.P. performed the artery ligation surgeries for the ischemia assays with assistance from M.T.R. P.C. provided the $Pgf^{-/-}$ mice. R.L.L., V.R.K. and B.A.C. wrote the manuscript.

Funding

This work was supported by awards from the Natural Sciences and Engineering Research Council, the Canada Research Chairs Program and the Canadian Foundation for Innovation to B.A.C. and by training awards from the Universidade Federal de Pernambuco and Conselho Nacional de Desenvolvimento Cientifico e Tecnologico (CNPq), Brazil to R.L.L.; Queen's University to V.R.K. and the Canadian Institutes of Health Research to M.T.R. The work of P.C. is supported by the Belgian Science Policy BELSPO—IUAP7/03, Structural funding by the Flemish Government—Methusalem funding, and the Flemish Science Fund—FWO grants.

Conflict of interest

None declared.

References

Aasa KL, Zavan B, Luna RL, Wong PG, Ventura NM, Tse YM, Carmeliet P, Adams MA, Pang SC, Croy BA. Placental growth factor influences maternal cardiovascular adaptation to pregnancy in mice. *Biol Reprod* 2015;**2**:1–10.

Autiero M, Waltenberger J, Communi D, Kranz A, Moons L, Lambrechts D, Kroll J, Plaisance S, De Mol M, Bono F *et al.* Role of PlGF in the intra- and intermolecular cross talk between the VEGF receptors Flt1 and Flk1. *Nat Med* 2003;**7**:936–943.

Baston-Buest DM, Porn AC, Schanz A, Kruessel JC, Janni W, Hess AP. Expression of the vascular endothelial growth factor receptor neuropilin-1 at the human embryo-maternal interface. *Eur J Obstet Gynecol Reprod Biol* 2011;**2**:151–156.

Beck H, Acker T, Püschel AW, Fujisawa H, Carmeliet P, Plate KH. Cell type-specific expression of neuropilins in an MCA-occlusion model in mice suggests a potential role in post-ischemic brain remodeling. *J Neuropathol Exp Neurol* 2002;**4**:339–350.

Bonnin A, Goeden N, Chen K, Wilson ML, King J, Shih JC, Blakely RD, Deneris ES, Levitt P. A transient placental source of serotonin for the fetal forebrain. *Nature* 2011;**7343**:347–350.

Cao Y. Positive and negative modulation of angiogenesis by VEGFR1 ligands. *Sci Signal* 2009;**59**:re1.

Carmeliet P, Moons L, Luttun A, Vincenti V, Compernolle V, De Mol M, Wu Y, Bono F, Devy L, Beck H *et al.* Synergism between vascular endothelial growth factor and placental growth factor contributes to angiogenesis and plasma extravasation in pathological conditions. *Nat Med* 2001;**5**:575–583.

Chaballe L, Schoenen J, Franzen R. Placental growth factor: a tissue modelling factor with therapeutic potentials in neurology? *Acta Neurol Belg* 2011; **1**:10–17.

Chappell JC, Mouillesseaux KP, Bautch VL. Flt-1 (vascular endothelial growth factor receptor-1) is essential for the vascular endothelial growth factor-Notch feedback loop during angiogenesis. *Arterioscler Thromb Vasc Biol* 2013;**8**:1952–1959.

Christinger HW, Fuh G, de Vos AM, Wiesmann C. The crystal structure of placental growth factor in complex with domain 2 of vascular endothelial growth factor receptor-1. *J Biol Chem* 2004;**11**:10382–10388.

Davis EF, Newton L, Lewandowski AJ, Lazdam M, Kelly BA, Kyriakou T, Leeson P. Pre-eclampsia and offspring cardiovascular health: mechanistic insights from experimental studies. *Clin Sci* 2012;**2**:53–72.

Degani S. Evaluation of fetal cerebrovascular circulation and brain development: the role of ultrasound and Doppler. *Semin Perinatol* 2009; **4**:259–269.

Dewerchin M, Carmeliet P. PlGF: a multitasking cytokine with disease-restricted activity. *Cold Spring Harb Perspect Med* 2012;**8**:1–24.

Dewerchin M, Carmeliet P. Placental growth factor in cancer. *Expert Opin Ther Targets* 2014;**11**:1339–1354.

Donnini S, Machein MR, Plate KH, Weich HA. Expression and localization of placenta growth factor and PlGF receptors in human meningiomas. *J Pathol* 1999;**1**:66–71.

Du H, Li P, Pan Y, Li W, Hou J, Chen H, Wang J, Tang H. Vascular endothelial growth factor signaling implicated in neuroprotective effects of placental growth factor in an in vitro ischemic model. *Brain Res* 2010;**1357**:1–8.

Duelsner A, Gatzke N, Glaser J, Hillmeister P, Li M, Lee EJ, Lehmann K, Urban D, Meyborg H, Stawowy P *et al.* Granulocyte colony-stimulating factor improves cerebrovascular reserve capacity by enhancing collateral growth in the circle of Willis. *Cerebrovasc Dis* 2012;**5**:419–429.

Errico M, Riccioni T, Iyer S, Pisano C, Acharya KR, Persico MG, De Falco S. Identification of placenta growth factor determinants for binding and activation of Flt-1 receptor. *J Biol Chem* 2004;**42**:43929–43939.

Fantin A, Vieira JM, Plein A, Maden CH, Ruhrberg C. The embryonic mouse hindbrain as a qualitative and quantitative model for studying the molecular and cellular mechanisms of angiogenesis. *Nat Protoc* 2013;**2**:418–429.

Freitas-Andrade M, Carmeliet P, Stanimirovic DB, Moreno M. VEGFR-2-mediated increased proliferation and survival in response to oxygen and glucose deprivation in PlGF knockout astrocytes. *J Neurochem* 2008; **3**:756–767.

Gaál EI, Tammela T, Anisimov A, Marbacher S, Honkanen P, Zarkada G, Leppänen VM, Tatlisumak T, Hernesniemi J, Niemelä M *et al.* Comparison of vascular growth factors in the murine brain reveals placenta growth factor as prime candidate for CNS revascularization. *Blood* 2013;**5**:658–665.

Goel A, Rana S. Angiogenic factors in preeclampsia: potential for diagnosis and treatment. *Curr Opin Nephrol Hypertens* 2013;**6**:643–650.

Goldstein JM, Seidman LJ, Horton NJ, Makris N, Kennedy DN, Caviness VS, Faraone SV, Tsuang MT. Normal sexual dimorphism of the adult human brain assessed by in vivo magnetic resonance imaging. *Cereb Cortex* 2001;**11**:490–497.

Gong G, He Y, Evans AC. Brain connectivity: gender makes a difference. *Neuroscientist.* 2011;**17**:575–591.

Harrington LS, Sainson RCA, Williams CK, Taylor JM, Shi W, Li JL, Harris AL. Regulation of multiple angiogenic pathways by Dll4 and Notch in human umbilical vein endothelial cells. *Microvasc Res* 2008;**2**:144–154.

Hayashi T, Noshita N, Sugawara T, Chan PH. Temporal profile of angiogenesis and expression of related genes in the brain after ischemia. *J Cereb Blood Flow Metab* 2003;**2**:166–180.

Hernández-Díaz S, Toh S, Cnattingius S. Risk of pre-eclampsia in first and subsequent pregnancies: prospective cohort study. *BMJ* 2009;**338**: b2255.

Herrera-Garcia G, Contag S. Maternal preeclampsia and risk for cardiovascular disease in offspring. *Curr Hypertens Rep* 2014;**9**:475.

Hiruma T, Nakajima Y. Development of pharyngeal arch arteries in early mouse embryo. *J Anat* 2002;**1**:15–29.

Kajantie E, Eriksson JG, Osmond C, Thornburg K, Barker DJP. Pre-eclampsia is associated with increased risk of stroke in the adult offspring the Helsinki birth cohort study. *Stroke* 2009;**4**:1176–1180.

Kalampokas E, Vrachnis N, Samoli E, Rizos D, Iliodromiti Z, Sifakis S, Kalampokas T, Vitoratos N, Creatsas G, Botsis D. Association of adiponectin and placental growth factor in amniotic fluid with second trimester fetal growth. *In Vivo* 2012;**2**:327–333.

Kaufman MH. *The Atlas of Mouse Development*, 2nd edn. London: Elsevier Academic Press, UK, 1992.

Krause DN, Duckles SP, Gonzales RJ. Local oestrogenic/androgenic balance in the cerebral vasculature. *Acta Physiol (Oxf)* 2011;**203**:181–186.

Lan N, Chiu MP, Ellis L, Weinberg J. Prenatal alcohol exposure and prenatal stress differentially alter glucocorticoid signaling in the placenta and fetal brain. *Neuroscience* 2015;pii:S0306-4522(15)00790-3.

Lowe R, Gemma C, Rakyan VK, Holland ML. Sexually dimorphic gene expression emerges with embryonic genome activation and is dynamic throughout development. *BMC Genomics* 2015;**16**:295.

Makrydimas G, Sotiriadis A, Savvidou MD, Spencer K, Nicolaides KH. Physiological distribution of placental growth factor and soluble Flt-1 in early pregnancy. *Prenat Diagn* 2008;**3**:175–179.

Muralimanoharan S, Maloyan A, Myatt L. Evidence of sexual dimorphism in the placental function with severe preeclampsia. *Placenta* 2013; **12**:1183–1189.

Papapostolou T, Briana DD, Boutsikou M, Iavazzo C, Puchner KP, Gourgiotis D, Marmarinos A, Malamitsi-Puchner A. Midtrimester amniotic fluid concentrations of angiogenic factors in relation to maternal, gestational and neonatal characteristics in normal pregnancies. *J Matern Fetal Neonatal Med* 2012;**1**:1–4.

Penn A, Koss W, Agrawal M, Volate S, Leuenberger D, Kiraly M, Pasca A, Chisholm K. Placental hormone contribution to fetal brain damage. *Placenta* 2014;**9**. A52.

Pipp F, Heil M, Issbrücker K, Ziegelhoeffer T, Martin S, Van Den Heuvel J, Weich H, Fernandez B, Golomb G, Carmeliet P *et al.* VEGFR-1-selective VEGF homologue PlGF is arteriogenic: evidence for a monocyte-mediated mechanism. *Circ Res* 2003;**4**:378–385.

Powers RW, Roberts JM, Plymire DA, Pucci D, Datwyler SA, Laird DM, Sogin DC, Jeyabalan A, Hubel CA, Gandley RE. Low placental growth factor across pregnancy identifies a subset of women with preterm preeclampsia type 1 versus type 2 preeclampsia? *Hypertension* 2012; **1**:239–246.

Proweller A, Wright AC, Horng D, Cheng L, Lu MM, Lepore JJ, Pear WS, Parmacek MS. Notch signaling in vascular smooth muscle cells is required to pattern the cerebral vasculature. *Proc Natl Acad Sci USA* 2007;**41**:16275–16280.

Ratsep MT, Felker AM, Kay VR, Tolusso L, Hofmann AP, Croy BA. Uterine natural killer cells: supervisors of vasculature construction in early decidua basalis. *Reproduction* 2015a;**2**:R91–R102.

Ratsep MT, Paolozza A, Hickman A, Maser B, Kay VR, Mohammad S, Pudwell J, Smith GN, Brien D, Stroman PW *et al.* Brain structural and vascular anatomy is altered in offspring of preeclamptic pregnancies: a pilot study. *Am J Neuroradiol.* 2015b (in press).

Romero R, Nien JK, Espinoza J, Todem D, Fu W, Chung H, Kusanovic JP, Gotsch F, Erez O, Mazaki-Tovi S *et al.* A longitudinal study of angiogenic (placental growth factor) and anti-angiogenic (soluble endoglin and soluble vascular endothelial growth factor receptor-1) factors in normal pregnancy and patients destined to develop preeclampsia and deliver a small for gestational age neonate. *J Matern Fetal Neonatal Med* 2008; **1**:9–23.

Ryan DJ, Byrne S, Dunne R, Harmon M, Harbison J. White matter disease and an incomplete circle of Willis. *Int J Stroke* 2013;**10**:1–6.

Staff AC, Braekke K, Harsem NK, Lyberg T, Holthe MR. Circulating concentrations of sFlt1 (soluble Fms-like tyrosine kinase 1) in fetal and maternal serum during pre-eclampsia. *Eur J Obstet Gynecol Reprod Biol* 2005;**1**:33–39.

Steenkiste CV, Ribera J, Geerts A, Pauta M, Tugues S, Casteleyn C, Libbrecht L, Olievier K, Schroyen B, Reynaert H *et al.* Inhibition of placental growth factor activity reduces the severity of fibrosis, inflammation, and portal hypertension in cirrhotic mice. *Hepatology* 2011;**5**:1629–1640.

Tontisirin N, Muangman SL, Suz P, Pihoker C, Fisk D, Moore A, Lam AM, Vavilala MS. Early childhood gender differences in anterior and posterior cerebral blood flow velocity and autoregulation. *Pediatrics* 2007; **119**:e610–e615.

Tuovinen S, Räikkönen K, Kajantie E, Pesonen AK, Heinonen K, Osmond C, Barker DJP, Eriksson JG. Depressive symptoms in adulthood and intrauterine exposure to pre-eclampsia: the Helsinki Birth Cohort Study. *BJOG* 2010;**10**:1236–1242.

Tuovinen S, Raikkonen K, Pesonen AK, Lahti M, Heinonen K, Wahlbeck K, Kajantie E, Osmond C, Barker DJP, Eriksson JG *et al.* Hypertensive disorders in pregnancy and risk of severe mental disorders in the offspring in adulthood: the Helsinki Birth Cohort Study. *J Psychiatr Res* 2012;**3**:303–310.

Tuovinen S, Eriksson JG, Kajantie E, Lahti J, Pesonen AK, Heinonen K, Osmond C, Barker DJP, Räikkönen K. Maternal hypertensive disorders in pregnancy and self-reported cognitive impairment of the offspring 70 years later: the Helsinki Birth Cohort Study. *Am J Obstet Gynecol* 2013; **3**:200.e1–200.e9.

Van Overbeeke JJ, Hillen B, Tulleken CA. A comparative study of the circle of Willis in fetal and adult life. The configuration of the posterior bifurcation of the posterior communicating artery. *J. Anat* 1991;**176**:45–54.

Vatten LJ, Eskild A, Nilsen TIL, Jeansson S, Jenum PA, Staff AC. Changes in circulating level of angiogenic factors from the first to second trimester as predictors of preeclampsia. *Am J Obstet Gynecol* 2007;**3**:1–6.

Xie D, Chen CC, Ptaszek LM, Xiao S, Cao X, Fang F, Ng HH, Lewin HA, Cowan C, Zhong S. Rewirable gene regulatory networks in the preimplantation embryonic development of three mammalian species. *Genome Res* 2010;**6**:804–815.

Xu Y, Luo J, Yue Z, Wu L, Zhang X, Zhou C, Zhao F, Wang X, Chen G. Increased expression of placental growth factor in patients with temporal lobe epilepsy and a rat model. *Brain Res* 2012a;**1429**:124–133.

Xu Y, Zhang Y, Guo Z, Yin H, Zeng H, Wang L, Luo J, Zhu Q, Wu L, Zhang X *et al.* Increased placental growth factor in cerebrospinal fluid of patients with epilepsy. *Neurochem Res* 2012b;**3**:665–670.

Yan C, Gong G, Wang J, Wang D, Liu D, Zhu C, Chen ZJ, Evans A, Zang Y, He Y. Sex- and brain size-related small-world structural cortical networks in young adults: a DTI tractography study. *Cereb Cortex* 2011; **21**:449–458.

Yang K, Banerjee S, Proweller A. Regulation of pre-natal circle of Willis assembly by vascular smooth muscle Notch signaling. *Dev Biol* 2013; **1**:107–120.

Zeng F, Baldwin DA, Schultz RM. Transcript profiling during preimplantation mouse development. *Dev Biol* 2004;**2**:483–496.